DALTON
FULL PAPER

Synthesis, structure, and reactivity of {(2-phosphinoethyl)silyl}-rhodium(I) complexes Rh[(κ²*Si*,*P*)-$Me_2Si(CH_2)_2PPh_2$]$(PMe_3)_n$ (n = 2, 3)

Masaaki Okazaki,* Shin Ohshitanai, Hiromi Tobita * and Hiroshi Ogino

Department of Chemistry, Graduate School of Science, Tohoku University, Sendai 980-8578, Japan

Received 1st February 2002, Accepted 19th February 2002
First published as an Advance Article on the web 5th April 2002

A (2-phosphinoethyl)silylrhodium(III) complex RhH(Cl)[(κ²*Si*,*P*)-$Me_2Si(CH_2)_2PPh_2$]$(PMe_3)_2$ (**1**) was synthesized by the thermal reaction of $RhCl(PMe_3)_n$ (n = 3, 4) with $HMe_2Si(CH)_2PPh_2$ at 50 °C for 2 h. Treatment of **1** with MeLi gave a coordinatively unsaturated rhodium(I) complex Rh[(κ²*Si*,*P*)-$Me_2Si(CH_2)_2PPh_2$]$(PMe_3)_2$ (**2**) which was possibly produced *via* transient formation of RhH(Me)[(κ²*Si*,*P*)-$Me_2Si(CH_2)_2PPh_2$]$(PMe_3)_2$ and subsequent reductive elimination of methane. X-Ray crystal structure analysis revealed that **2** adopts a slightly distorted square planar geometry. When the reaction of **1** with MeLi was carried out in the presence of PMe_3, a coordinatively saturated silylrhodium(I) complex Rh[(κ²*Si*,*P*)-$Me_2Si(CH_2)_2PPh_2$]$(PMe_3)_3$ (**3**) was formed. According to the X-ray crystal structure analysis, **3** adopts a five-coordinate, slightly distorted trigonal-bipyramidal arrangement in which the silyl silicon atom and a PMe_3 ligand occupy the axial positions. Variable temperature NMR measurements revealed that both **2** and **3** undergo the exchange of PMe_3 ligands on the NMR timescale. The exchange in **2** is intramolecular, while that in **3** is intermolecular. Treatment of $HSiMe_2Ph$ with **2** gave rise to selective dehydrogenative coupling of hydrosilanes to afford $(SiMe_2Ph)_2$ and RhH_2[(κ²*Si*,*P*)-$Me_2SiCH_2CH_2PPh_2$]$(PMe_3)_2$ (**5**).

Introduction

Wilkinson-type complexes $RhCl(PR_3)_3$ have been employed as active homogeneous catalysts for various transformation reactions of organic compounds.[1] Introduction of silyl ligands in place of chlorine ligands could enhance or change the reactivity and catalytic performance of transition metal complexes, because silyl ligands exhibit an exceptionally strong σ-donor character and high *trans*-influencing ability.[2] Although silylrhodium(I) complexes are somewhat rare, a few compounds of the type L_nRhSiR_3 (L = tertiary phosphine) have been synthesized.[3,4,5,6,7] The first structurally characterized silylrhodium(I) complex has been reported by Stobart.[3] Treatment of Rh(tripsi)H(Cl) with MeLi under a CO atmosphere gave Rh(tripsi)(CO) *via* reductive elimination of methane (tripsi = $Si(CH_2CH_2PPh_2)_3$). Milstein *et al.* reported the activation of carbon–fluorine bonds by the coordinatively unsaturated rhodium(I) complex L_3RhSiR_3 (L = PMe_3, R_3 = Me_2Ph, Ph_3):[4] the Rh(I) silyl complex reacts quantitatively with C_6F_6 at room temperature to give $L_3RhC_6F_5$ and R_3SiF. This experimental result indicates that Rh(I) silyl complexes are potentially applicable to active catalysts. However, facile elimination of silyl ligands from the metal center has retarded the progress of such application. Thorn and Harlow reported studies on the reactivity of $L_3RhSiPh_3$ (L = PMe_3).[5] When the solution of the Rh(I) silyl complex is exposed to ethylene, carbon–silicon bond formation occurs readily to give $(CH_2{=}CH)SiPh_3$ and unidentified product(s) containing rhodium. This reaction may proceed *via* olefin insertion into a rhodium–silicon bond and subsequent β-hydrogen elimination. The Rh(I) silyl complex also reacted with excess methyl iodide to form $MeSiPh_3$ and *mer*-$L_3I_2RhCH_3$. A plausible formation mechanism of these products involves the transient formation of the Rh(III) iodo(methyl)(silyl) complex $L_3RhI(CH_3)(SiPh_3)$. Subsequently, reductive elimination of $MeSiPh_3$ and oxidative addition of MeI occur to give the final products. To suppress such elimination of silyl ligands, chelate-type (2-phosphinoethyl)silyl ligands have been employed.[6] We report here the synthesis, crystal structure, and properties of coordinatively unsaturated and saturated Rh(I) silyl complexes Rh[(κ²*Si*,*P*)-$Me_2Si(CH_2)_2PPh_2$]$(PMe_3)_n$ (n = 2, 3). Reactions of these Rh(I) silyl complexes with monohydrosilane were also examined. A part of this work has been published as a preliminary communication.[7]

Results and discussion

Synthesis of RhCl(H)[(κ²*Si*,*P*)-$Me_2Si(CH_2)_2PPh_2$]$(PMe_3)_2$ (1)

The rhodium(III) complex RhCl(H)[(κ²*Si*,*P*)-$Me_2Si(CH_2)_2PPh_2$]$(PMe_3)_2$ (**1**) can be readily prepared by the thermal reaction shown in eqn. 1. Workup and recrystallization from

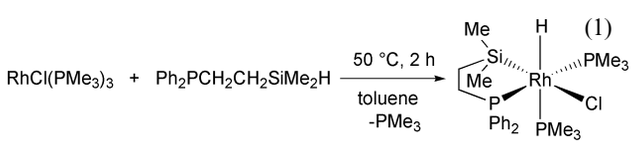

(1)

1

toluene–hexane at −10 °C afforded ivory crystals in 90% yield. The ^1H, ^{13}C, ^{29}Si, and ^{31}P NMR spectral data established that **1** possesses chloro, hydrido, and silyl ligands in a *mer*-relationship. The ^1H resonance of Rh–H appears at −9.32 ppm as double quartets by coupling with one *trans*-^{31}P nucleus (^2J(PH) = 158 Hz) and one ^{103}Rh (^1J(RhH) = 15 Hz) and two *cis*-^{31}P nuclei (^2J(PH) = 15 Hz). The coupling pattern of the ^{31}P resonances indicates that three phosphorus atoms are located in a *mer*-relationship. In the $^{29}Si\{^1H\}$ NMR spectrum, the signal appears at 40.4 ppm as a dddd by coupling with ^{103}Rh (^1J(RhSi) = 26.1 Hz) and three *cis*-^{31}P nuclei (^2J(PSi) = 10.5, 8.2, 6.9 Hz).

The ORTEP drawing of **1** is shown in Fig. 1. Selected bond distances and angles are listed in Table 1. The complex adopts a six-coordinate, slightly distorted octahedral arrangement in which three phosphorus atoms are located in a *mer*-relationship

Table 1 Selected bond distances (Å) and angles (°) for RhCl(H)-[(κ²*Si*,*P*)-$Me_2Si(CH_2)_2PPh_2$](PMe_3)$_2$ (**1**)

Rh–Cl	2.535(1)	Rh–P1	2.2925(9)
Rh–P2	2.306(1)	Rh–P3	2.366(1)
Rh–Si	2.331(1)	Rh–H	1.71(8)
P1–C2	1.823(4)	P1–C5	1.822(4)
P1–C11	1.837(4)	P2–C17	1.814(5)
P2–C18	1.827(5)	P2–C19	1.818(5)
P3–C20	1.822(4)	P3–C21	1.815(4)
P3–C22	1.822(4)	Si–C1	1.902(4)
Si–C3	1.888(5)	Si–C4	1.883(4)
C1–C2	1.542(6)		
Cl–Rh–P1	90.45(3)	Cl–Rh–P2	88.20(4)
Cl–Rh–P3	92.31(4)	Cl–Rh–Si	171.08(4)
P1–Rh–P2	160.37(4)	P1–Rh–P3	102.52(3)
P1–Rh–Si	85.10(4)	P2–Rh–P3	97.10(4)
P2–Rh–Si	93.39(4)	P3–Rh–Si	96.20(4)

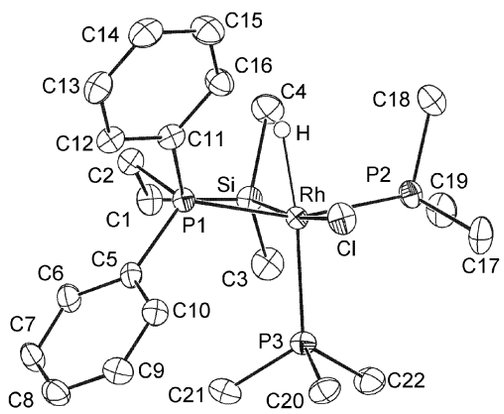

Fig. 1 ORTEP drawing of RhH(Cl)[(κ²*Si*,*P*)-$Me_2Si(CH_2)_2PPh_2$]-(PMe_3)$_2$ (**1**).

in accord with the above-mentioned characterization by NMR spectroscopy. The Rh–H hydrogen atom was located by the difference Fourier synthesis and refined isotropically. The bond distance of Rh–H (1.71(8) Å) is reasonable compared with those in previously reported hydridorhodium(III) complexes. A strongly *trans*-influencing silyl group is located *trans* to the weakly *trans*-influencing chlorine ligand. The Rh–Si bond length (2.331(1) Å) lies in the normal range of those in the previously reported electron-rich silylrhodium(III) complexes.[8] The bite angle of Si–Rh–P1 (85.10°) is characteristic of those in the complexes containing five-membered (2-phosphinoethyl)silyl chelate ligands.[6]

The reaction of $RhCl(PMe_3)_3$ with $HSiPh_3$ was reported by Osakada *et al*.[8] The reaction proceeded at room temperature to give *mer*-$RhH(Cl)(SiPh_3)(PMe_3)_3$. The complex adopts a geometry similar to **1** in which three phosphorus atoms are mutually meridional and the silyl ligand is located at the *trans*-position of the chlorine ligand. Importantly, in the reaction of $RhCl(PMe_3)_3$ with $HSiPh_3$, the oxidative addition of Si–H is reversible, whereas in eqn. 1 the process takes place irreversibly undoubtedly owing to the chelate effect of the (2-phosphinoethyl)silyl ligand.

Synthesis of Rh[(κ²*Si*,*P*)-$Me_2Si(CH_2)_2PPh_2$](PMe_3)$_2$ (2)

It has been known that chloro(hydrido) complexes $L_nMCl(H)$ reacted with a base such as an amine to give a coordinatively unsaturated complex *via* elimination of HCl.[9] We therefore attempted the reaction of RhH(Cl)[(κ²*Si*,*P*)-$Me_2Si(CH_2)_2PPh_2$]-(PMe_3)$_2$ (**1**) with NEt_3 which was monitored spectroscopically. However, no reaction was observed, even at 80 °C.

Treatment of **1** with 1 equiv. of MeLi in toluene at room temperature resulted in nearly quantitative formation of a coordinatively unsaturated silylrhodium(I) complex Rh-[(κ²*Si*,*P*)-$Me_2Si(CH_2)_2PPh_2$](PMe_3)$_2$ (**2**) (eqn. 2). Workup of the resulting solution and recrystallization from toluene at −75 °C gave orange crystals of **2** in 35% isolated yield. The structure of **2** has been determined by spectroscopic and analytical methods and by X-ray crystal structure analysis.

Table 2 Selected bond distances (Å) and angles (°) for Rh[(κ²*Si*,*P*)-$Me_2Si(CH_2)_2PPh_2$](PMe_3)$_2$ (**2**)

Rh–P1	2.2672(7)	Rh–P2	2.2823(7)
Rh–P3	2.3339(7)	Rh–Si	2.3937(8)
P1–C4	1.840(3)	P1–C5	1.839(3)
P1–C11	1.843(3)	P2–C17	1.832(3)
P2–C18	1.840(3)	P2–C19	1.851(3)
P3–C20	1.840(3)	P3–C21	1.841(3)
P3–C22	1.827(3)	Si–C1	1.903(3)
Si–C2	1.919(3)	Si–C3	1.906(3)
C3–C4	1.519(4)		
P1–Rh–P2	167.65(3)	P1–Rh–P3	95.96(3)
P1–Rh–Si	81.24(3)	P2–Rh–P3	95.13(3)
P2–Rh–Si	87.85(3)	P3–Rh–Si	176.58(2)

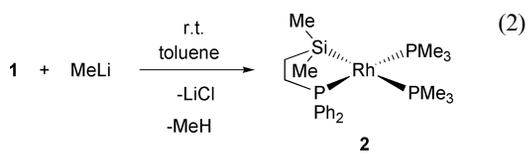

(2)

The square planar complex **2** is fluxional in $C_6D_5CD_3$ at room temperature (Fig. 2). In the ^1H NMR spectrum at −40 °C, the two PMe_3 ligands appear inequivalently at 0.80 and 1.32 ppm. When the temperature is raised, these signals gradually broaden, coalesce, and finally become a slightly broad signal at 1.08 ppm (20 °C). In the $^{31}P\{^1H\}$ NMR spectrum at −40 °C, three sets of signals appear at −21.1, −9.0, and 70.5 ppm which are assigned to PMe_3 *trans* to the silyl group, PMe_3 *trans* to PPh_2, and PPh_2, respectively. When the temperature is raised, the two signals at −21.1 and −9.0 ppm assigned to two PMe_3 ligands gradually broaden, coalesce, and finally become a broad triplet at 20 °C. At 20 °C, the signal of the PPh_2 moiety does not lose the coupling with two PMe_3 ligands and appears at 70.4 ppm as double triplets coupled with ^{103}Rh (^1J(RhP) = 160 Hz) and two ^{31}P nuclei (^2J(PP) = 131 Hz). These spectroscopic features are consistent with the intramolecular exchange of two PMe_3 ligands. Muetterties *et al.* studied the dynamic behavior of $Rh(CH_2Ph)(PMe_3)_3$ by variable-temperature NMR spectroscopy.[10] At 60 °C, the PMe_3 resonances become equivalent and they lose their coupling with the ^{103}Rh nuclei. The observations are consistent with a fluxional process resulting from the intermolecular PMe_3 exchange. The reason for the difference in the exchange process of PMe_3 ligands between the (2-phosphinoethyl)silyl complex **2** and the benzyl complex is obscure at present. The ^{29}Si resonance appears at 42.3 ppm at 20 °C.

The ORTEP drawing of **2** is shown in Fig. 3. Selected bond distances and angles of **2** are listed in Table 2. Complex **2** is among a few coordinatively unsaturated silylrhodium(I) complexes.[4,5,11] The angles of P1–Rh–P2 and P3–Rh–Si are 167.65(3) and 176.58(2)°, respectively, indicating a slightly distorted square planar coordination geometry of **2**. The Rh–Si bond length is 2.3937(8) Å which is relatively longer than those of the previously reported coordinatively unsaturated silylrhodium(I) complexes $(Ph_3Si)Rh(PMe_3)_3$ (2.317(1) Å)[5] and $(PhMe_2Si)Rh(PMe_3)_3$ (2.3804(10) Å).[11a] The change of the Rh–Si bond lengths is ascribable to the degree of the M(dπ)–SiX(σ*) interaction.[12] When more electron-withdrawing groups are bonded to silicon, this interaction becomes stronger and, as a result, the Rh–Si bond becomes shorter. The silyl ligand in **2** bears three electron-releasing alkyl groups on the silicon atom which make the Rh–Si bond of **2** the longest among them. In

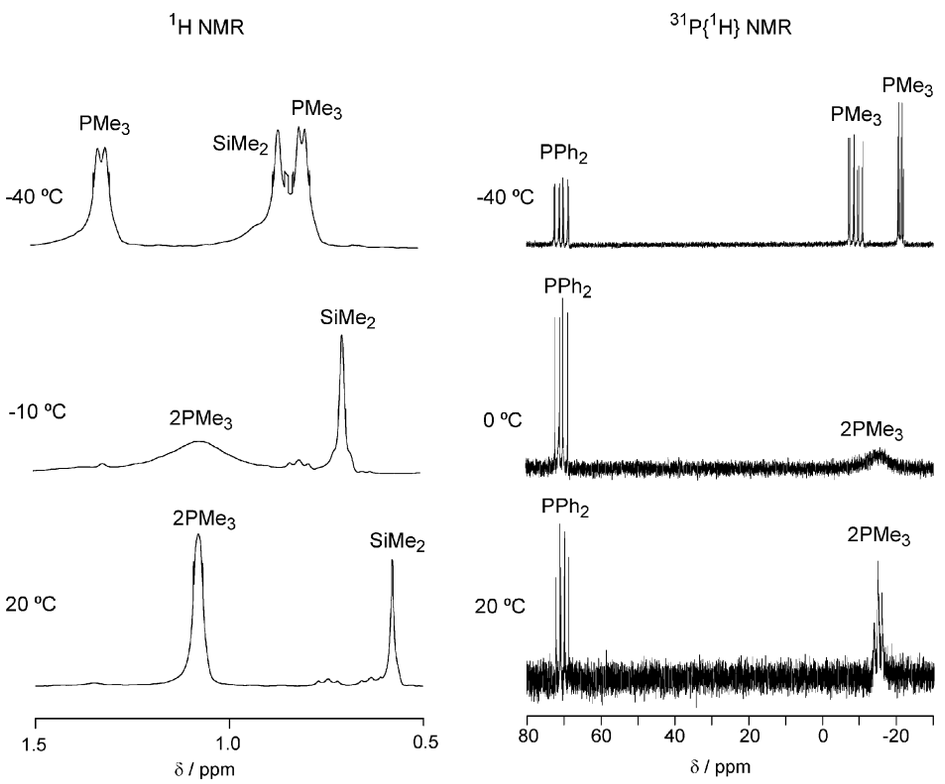

Fig. 2 Variable-temperature ^{1}H (300 MHz, toluene-d_8) and ^{31}P{^{1}H} NMR (121.5 MHz, toluene-d_8) spectra of Rh[(κ^2*Si*,*P*)-$Me_2Si(CH_2)_2PPh_2$]-$(PMe_3)_2$ (**2**).

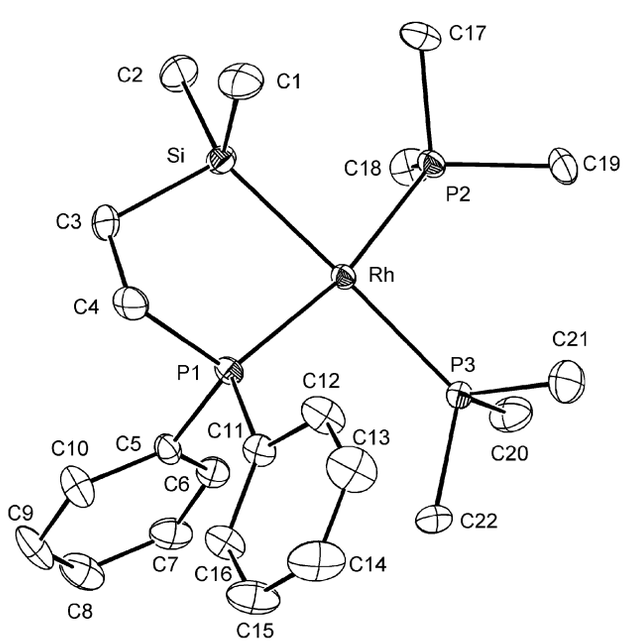

Fig. 3 ORTEP drawing of Rh[(κ^2*Si*,*P*)-$Me_2Si(CH_2)_2PPh_2$]$(PMe_3)_2$ (**2**).

good agreement with the strong *trans*-influence expected to the silyl ligand in **2**,[2c] the bond length of Rh–P3, which is *trans* to the silyl ligand, is about 0.04 Å longer than those of Rh–P1 and Rh–P2.

When the reaction of **1** with excess MeLi was carried out, initial formation of **2** was confirmed spectroscopically. However, further reaction occurred to give the PMe_3-adduct of **2** Rh[(κ^2*Si*,*P*)-$Me_2Si(CH_2)_2PPh_2$]$(PMe_3)_3$ (**3**) in 30% isolated yield. Although the formation mechanism of **3** by the reaction of the intermediate **2** with MeLi is not clear, it would involve generation of the anionic complex $Li^+[\mathbf{2}]^-$ resulting from the electron-transfer reaction between **2** and MeLi. The anion $Li^+[\mathbf{2}]^-$ releases a PMe_3 molecule, which is then ligated by **2**. It is well known that the substitution reaction is accelerated in the presence of reductant or oxidant *via* generation of 17 and 19-electron species.[13]

Synthesis of Rh[(κ^2*Si*,*P*)-$Me_2Si(CH_2)_2PPh_2$]$(PMe_3)_3$ (3)

When the reaction of **1** with MeLi was performed in the presence of PMe_3, Rh[(κ^2*Si*,*P*)-$Me_2Si(CH_2)_2PPh_2$]$(PMe_3)_3$ (**3**) was formed in an almost quantitative yield (eqn. 3). Workup

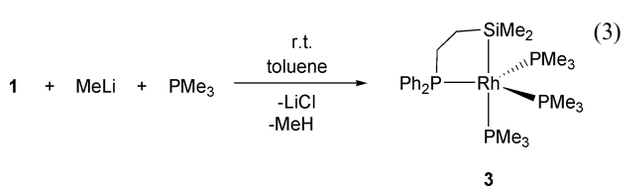

(3)

and recrystallization from toluene at −75 °C gave orange crystals of **3** (74% yield). The structure of **3** has been determined using spectroscopic and elemental analysis data and by X-ray crystal structure analysis. Complex **3** is much more stable than the unsaturated complex **2**.

A variable-temperature ^{31}P NMR study of **3** suggests the existence of a fluxional behavior of three PMe_3 ligands. Three broad signals are observed at −24.0, −13.9, and 65.8 ppm in the ^{31}P{^{1}H} NMR at 20 °C. Cooling of the solution gives rise to the sharpening of these signals, and at −30 °C, they become three sharp multiplets coupled with ^{31}P and ^{103}Rh nuclei at −22.8, −13.1, and 65.7 ppm, in an approximate intensity ratio of 2 : 1 : 1. These can be assigned to two equatorial PMe_3, one axial PMe_3, and PPh_2, respectively. As the temperature is raised, two multiplet signals at −24.0 and −13.9 ppm gradually broaden and coalesce. At 60 °C, the signal of PPh_2 loses the coupling with three PMe_3 ligands and appears as a broad doublet (^1J(RhP) = 158 Hz) at 66.8 ppm. The ^{31}P resonance for one axial and two equatorial PMe_3 ligands appears as one broad signal at −20.4 ppm. These coupling patterns of ^{31}P

resonances are consistent with the intermolecular exchange process of three PMe_3 ligands in the trigonal-bipyramidal complex (eqn. 4).

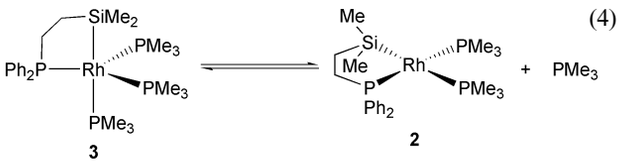

(4)

The intermolecular exchange process of PMe_3 ligands in **3** was also confirmed by a variable temperature $^{31}P\{^1H\}$ NMR study on the mixture of **3** and PMe_3 (Fig. 4). At 25 °C,

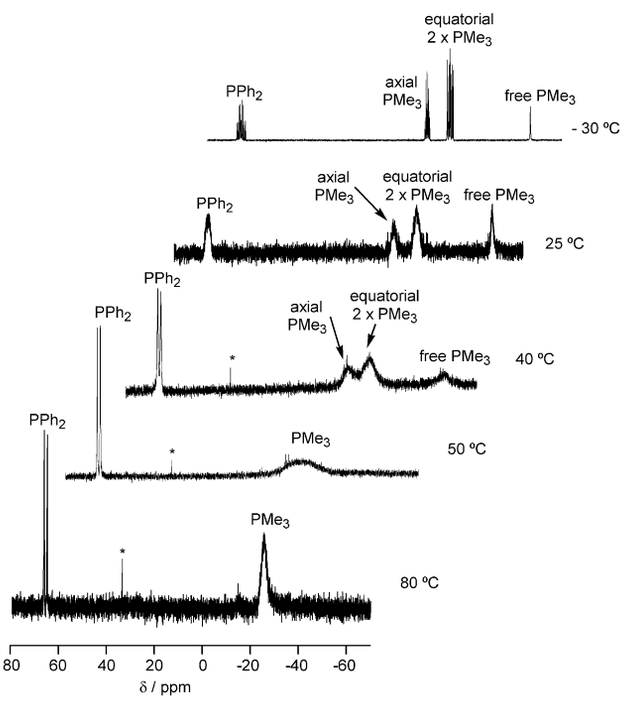

Fig. 4 Variable temperature $^{31}P\{^1H\}$ NMR (121.5 MHz, toluene-d_8) spectrum of a mixture of Rh[(κ^2*Si*,*P*)-$Me_2Si(CH_2)_2PPh_2$]$(PMe_3)_2$ (**3**) and PMe_3 (* impurity).

four separate broad signals appear at 65.6, −14.5, −24.3, and −56.8 ppm, assignable to PPh_2, axial PMe_3, equatorial PMe_3, and free PMe_3, respectively. Cooling of the solution to −30 °C gave four sharp signals at 65.7, −13.1, −22.8, and −56.8 ppm, where the exchange of PMe_3 is inhibited on the NMR timescale. When the temperature is raised, three broad signals of PMe_3 at −13.1, −22.8, and −56.7 ppm gradually broaden and coalesce. At 80 °C, two separate resonances are present: one is a sharp doublet at 66.1 ppm (PPh_2, ^1J(RhP) = 160 Hz) without the coupling with PMe_3 and the other is a broad signal at −25.3 ppm (PMe_3). These observations are also consistent with the mechanism involving the intermolecular exchange of PMe_3 ligands *via* formation of square-planar **2**. The previously reported Rh(I) silyl and methyl complexes of the type $RhRL_4$ (R = Me,[10] $SiHPh_2$,[14] L = PMe_3) with a trigonal-bipyramidal geometry also exhibit the intermolecular exchange of PMe_3 ligands. In contrast, the iridium(I) complexes $IrMe(PMe_3)_4$[15] and Ir[(κ^2*Si*,*P*)-$Me_2Si(CH_2)_2PPh_2$]$(PMe_3)_3$[16] exhibit the intramolecular exchange of PMe_3 ligands on the NMR timescale. These differences would be attributable to the strength of metal–phosphorus bonds.[17] In general, the iridium–phosphorus bond is stronger than the rhodium–phosphorus bond.

The ORTEP drawing of **3** is shown in Fig. 5. Selected bond distances and angles of **3** are listed in Table 3. The complex **3** adopts a five-coordinate, slightly distorted trigonal-bipyramidal structure in which the silyl silicon atom and a

Table 3 Selected bond distances (Å) and angles (°) for Rh[(κ^2*Si*,*P*)-$Me_2Si(CH_2)_2PPh_2$]$(PMe_3)_3$ (**3**)

Rh–P1	2.2836(9)	Rh–P2	2.3241(8)
Rh–P3	2.3099(9)	Rh–P4	2.3488(9)
Rh–Si	2.405(1)	P1–C4	1.853(4)
P1–C5	1.850(4)	P1–C11	1.860(4)
P2–C17	1.843(4)	P2–C18	1.853(4)
P2–C19	1.835(4)	P3–C20	1.846(4)
P3–C21	1.846(3)	P3–C22	1.844(4)
P4–C23	1.838(4)	P4–C24	1.844(3)
P4–C25	1.832(4)	Si–C1	1.913(4)
Si–C2	1.906(4)	Si–C3	1.904(4)
C3–C4	1.522(5)		
P1–Rh–P2	118.35(3)	P1–Rh–P3	130.51(3)
P1–Rh–P4	91.32(3)	P1–Rh–Si	80.18(3)
P2–Rh–P3	109.46(3)	P2–Rh–P4	99.45(3)
P2–Rh–Si	91.50(3)	P3–Rh–P4	92.94(3)
P3–Rh–Si	86.78(3)	P4–Rh–Si	168.45(3)

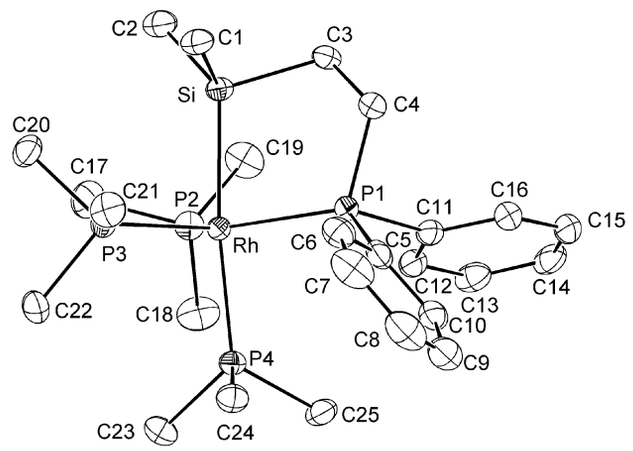

Fig. 5 ORTEP drawing of Rh[(κ^2*Si*,*P*)-$Me_2Si(CH_2)_2PPh_2$]$(PMe_3)_3$ (**3**).

PMe_3 ligand occupy the axial positions while the PPh_2 moiety and two PMe_3 ligands are located in equatorial sites. The Rh–Si bond length is 2.405(1) Å which is somewhat longer than that of the previously reported silylrhodium(I) complex Rh(η^4-Si-$(CH_2CH_2PPh_2)_3$)(CO) (2.379(5) Å) in which the silicon atom and a CO ligand are located in the axial positions.[3] The lengthening of the Rh–Si bond may be due to the stronger σ-donating ability of the tertiary phosphine ligand compared to the CO ligand.

In a previous paper, we reported the synthesis and properties of iridium(I) and iridium(III) complexes having the (2-phosphinoethyl)silyl chelate ligand.[16] The iridium analog of **1**, IrCl(H)[(κ^2*Si*,*P*)-$Me_2Si(CH_2)_2PPh_2$]$(PMe_3)_3$ (**1-Ir**), was synthesized by the thermal reaction of $[Ir(CO)(PMe_3)_4]Cl$ with $HMe_2Si(CH_2)_2PPh_2$ at 80 °C. The iridium complex **1-Ir** has the same geometry as the rhodium analog **1**. The reaction of **1-Ir** with MeLi was carried out under conditions similar to those described in eqn. 2. It afforded the iridium(III) complex IrMe(H)[(κ^2*Si*,*P*)-$Me_2Si(CH_2)_2PPh_2$]$(PMe_3)_3$, the rhodium(III) analog of which was not detected in the reaction of **1** with MeLi. Thermolysis of the iridium(III) complex in toluene at 55 °C led to elimination of methane to give the unidentified product(s) with an Ir–H bond. No formation of Ir[(κ^2*Si*,*P*)-$Me_2Si(CH_2)_2PPh_2$]$(PMe_3)_2$ (**2-Ir**) was observed. This striking difference in the thermal stability between Rh and Ir complexes is consistent with the general trend: The iridium complexes with the metal center in high oxidation state III are more stable than the corresponding rhodium complexes.[18] When the thermal reaction of **2-Ir** was carried out in the presence of PMe_3, a coordinatively saturated silyliridium(I) complex Ir[(κ^2*Si*,*P*)-$Me_2Si(CH_2)_2PPh_2$]$(PMe_3)_3$ (**3-Ir**) was formed, which adopts the trigonal-bipyramidal geometry with the silyl and PMe_3 groups in the axial positions.

Reactions of Rh[(κ²*Si*,*P*)-$Me_2Si(CH_2)_2PPh_2$]$(PMe_3)_n$ (n = 2 (2), 3 (3)) with monohydrosilane

Complex **2** represents the first example of a coordinatively unsaturated trialkylsilylrhodium(I) complex. Due to the strongly electron-releasing character of the trialkylsilyl moiety, **2** is expected to be highly reactive toward various small molecules. In fact, the reaction of **2** with 6 equiv. of $HSiMe_2Ph$ proceeded spontaneously at room temperature to give a hydrido(silyl)-rhodium(III) complex **4** almost quantitatively, although isolation of **4** was not successful due to its thermal instability (eqn. 5). The presence of both Rh–H (δ −10.30, 1H) and Rh–SiMe_2Ph (δ 0.45, 6H) resonances in the ^{1}H NMR spectrum at −20 °C supports the structure shown in eqn. 5. The coupling pattern of the ^{31}P NMR spectrum established the geometry of **4** in which three phosphorus atoms are located at mutually *fac*-positions. After 20 h at room temperature, the mixture of **4** and $HSiMe_2Ph$ was converted to dihydrido complex RhH_2[(κ²*Si*,*P*)-$Me_2Si(CH_2)_2PPh_2$]$(PMe_3)_2$ (**5**) and $(SiMe_2Ph)_2$ in 91% yield each (eqn. 5). Characterization of $(SiMe_2Ph)_2$ was based on com-

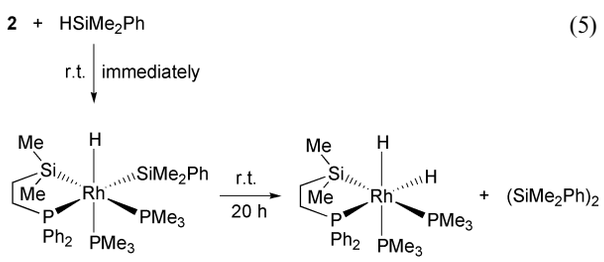

parison of the ^{1}H, ^{13}C, and ^{29}Si NMR spectra with the authentic sample synthesized by the published procedure.[22] The dihydrido complex **5** was independently synthesized by treatment of **3** with H_2 in 63% yield. It shows characteristic IR absorption bands due to ν(Rh–H) vibrations at 1929 and 1884 cm^{-1}. The presence of two inequivalent hydrido ligands was confirmed by the ^{1}H NMR spectrum, which shows two hydrido peaks at δ −10.57 and −9.27. The coupling pattern of two hydrido peaks with three ^{31}P and one ^{103}Rh nuclei supports the geometry shown in eqn. 5, which is confirmed by the ^{31}P and ^{29}Si NMR data.

Reaction of a coordinatively saturated silylrhodium(I) complex Rh[(κ²*Si*,*P*)-$Me_2Si(CH_2)_2PPh_2$]$(PMe_3)_3$ (**3**) with $HSiMe_2Ph$ was also examined. Treatment of **3** with 5 equiv. $HSiMe_2Ph$ in C_6D_6 at room temperature afforded a mixture of **3**, **4**, and free PMe_3. After 89 h at room temperature, only a trace amount of $(SiMe_2Ph)_2$ was formed and further reaction at 80 °C for 1 week led to the decomposition of **3** and **4**.

A plausible mechanism for the formation of **5** and $(SiMe_2Ph)_2$ is illustrated in Scheme 1. This mechanism firstly involves the formation of **4** *via* oxidative addition of $HSiMe_2Ph$. The next step is the dissociation of PMe_3 from **4** and then oxidative addition of $HSiMe_2Ph$ takes place to give a silylrhodium(V) intermediate $RhH_2(SiMe_2Ph)_2$[(κ²*Si*,*P*)-$Me_2SiCH_2CH_2PPh_2$](PMe_3) (**A**). A silylrhodium(V) complex analogous to **A** has been reported by Nagashima *et al.*[19] Complex **A** undergoes reductive elimination of $(SiMe_2Ph)_2$ and subsequent ligation of PMe_3 to Rh gives **5**. In the reaction of **3** with $HSiMe_2Ph$, the resulting free PMe_3 retards the further dissociation of a PMe_3 ligand from **4**.

As mentioned above, Osakada *et al.* reported the reaction of $RhCl(PMe_3)_3$ with $HSiAr_3$.[8] The reaction proceeded at room temperature to give the Si–H oxidative addition product *mer*-[$RhCl(H)(SiAr_3)(PMe_3)_3$] (Fig. 6). In this reaction, Si–Si reductive coupling products such as $RhCl(H)_2(PMe_3)_3$ and $(SiAr_3)_2$ were not observed. Thus, the reaction in eqn. 5 is characteristic of a coordinatively unsaturated silylrhodium(I) complex **2**. The dramatic difference in reactivity between **2** and $RhCl(PMe_3)_3$ is of great interest. This difference is attributable to the exceptionally strong *trans*-effect of the silyl ligand in intermediate **4**.[20] Further reaction of **4** and *mer*-[$RhCl(H)(SiAr_3)(PMe_3)_3$] requires the dissociation of a PMe_3 ligand, which allows it to form bis(silyl)rhodium(V) intermediates. In complex **4**, the highly *trans*-effecting silyl moiety of (2-phosphinoethyl)silyl chelate ligand would accelerate the dissociation of the *trans*-PMe_3 ligand, while such an effect is not operative in *mer*-[$RhCl(H)(SiAr_3)(PMe_3)_3$].

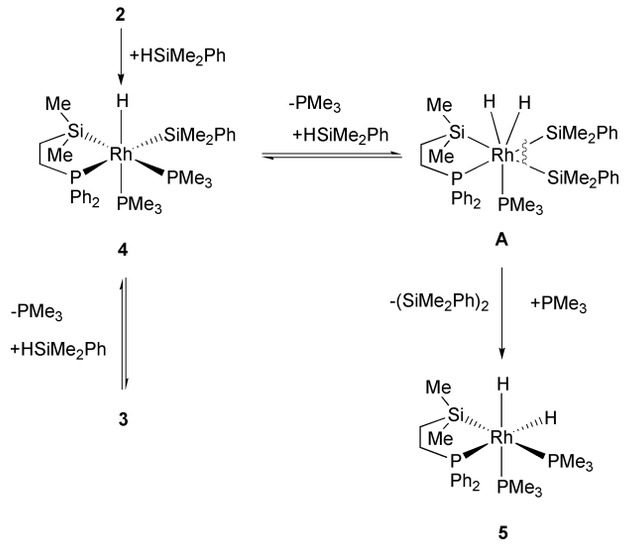

Scheme 1

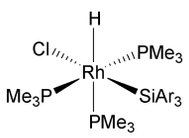

Fig. 6 Geometry of *mer*-[$RhCl(H)(SiAr_3)(PMe_3)_3$].

It has been known that the dehydrogenative coupling of monohydrosilanes requires considerably severe conditions and is accompanied by the scrambling of substituents on the silicon atoms.[21] It should be noted that the reaction (eqn. 5) proceeds at room temperature to give the silicon–silicon coupling product exclusively without the formation of the scrambling products.

Conclusions

We have synthesized the novel silylrhodium(I) complexes Rh[(κ²*Si*,*P*)-$Me_2Si(CH_2)_2PPh_2$]$(PMe_3)_2$ (**2**) and Rh[(κ²*Si*,*P*)-$Me_2Si(CH_2)_2PPh_2$]$(PMe_3)_3$ (**3**). The structures of **2** and **3** were determined by NMR spectroscopy and X-ray crystal structure analysis. Complex **2** adopts a square-planar geometry and exhibits the intramolecular exchange of PMe_3 ligands. Complex **3** adopts a trigonal-bipyramidal geometry with the silyl moiety and a PMe_3 ligand occupying the axial positions. Complex **3** undergoes an intermolecular exchange process of PMe_3 ligands and generates the coordinatively unsaturated **2** under mild conditions.

Dehydrogenative coupling of monohydrosilanes can be mediated by the coordinatively unsaturated silylrhodium(I) complex **2**. This novel reactivity seems to result from the strong *trans*-effect character of silyl ligands. Introduction of (phosphinoethyl)silyl ligands would open up rich chemistry.

Experimental

General procedures

All manipulations were carried out under a dry nitrogen atmosphere. Reagent-grade toluene and hexane were distilled from sodium-benzophenone ketyl immediately before use.

Benzene-d_6 and toluene-d_8 were dried over a potassium mirror and transferred into an NMR tube under vacuum. $HMe_2Si(CH_2)_2PPh_2$ [23] and $[Rh(\mu\text{-}Cl)(COD)]_2$ [24] were prepared according to literature methods. Other chemicals were purchased from Wako Pure Chemical Industries, Ltd., and used as received. All NMR data were recorded on a Bruker ARX-300 spectrometer. ^{29}Si NMR spectra were obtained by the DEPT pulse sequence. IR spectra were recorded on a Horiba FT-200 spectrometer.

RhH(Cl)[(κ^2*Si*,*P*)-$Me_2Si(CH_2)_2PPh_2$](PMe_3)$_2$ (1)

To a toluene solution (30 mL) of $RhCl(PMe_3)_n$ (n = 3, 4), prepared by refluxing the THF solution of $[Rh(\mu\text{-}Cl)(COD)]_2$ (699 mg, 1.42 mmol) (COD = 1,5-cyclooctadiene) and PMe_3 (1.0 mL, d = 0.748 g cm^{-3}, 9.80 mmol) for 14 h, was added dropwise $HSiMe_2(CH_2)_2PPh_2$ (979 mg, 3.59 mmol). After addition was complete, the mixture was stirred for 2 h at 50 °C. Removal of volatiles under reduced pressure resulted in a pale yellow oily residue, which was extracted with toluene (10 mL × 3). The extract was filtered through a Celite pad and concentrated under reduced pressure. Recrystallization of the residue from toluene–hexane at −10 °C gave ivory crystals of RhH(Cl)-[(κ^2*Si*,*P*)-$Me_2Si(CH_2)_2PPh_2$](PMe_3)$_2$ (**1**) (1.44 g, 2.56 mmol, 90% based on Rh). ^{1}H NMR (300 Hz, C_6D_6): δ −9.32 (dq, $^2J(P_{trans}H)$ = 158 Hz, $^2J(P_{cis}H)$ = ^1J(RhH) = 15 Hz, 1H, RhH), 0.23 (s, 3H, SiMe), 0.38 (s, 3H, SiMe), 0.80 (d, ^2J(PH) = 6.9 Hz, 9H, PMe_3 (*trans* to RhH), 0.83 (m, 2H, $SiCH_2$), 1.47 (dd, ^2J(PH) = 8.9 Hz, ^3J(PH) = 2.1 Hz, PMe_3 (*trans* to PPh_2), 2.08 (m, 2H, PCH_2), 6.95–7.11 (m, 6H, *m,p*-Ph), 8.15, 8.30 (m, 2H × 2, *o*-Ph). $^{13}C\{^1H\}$ NMR (75.5 MHz, C_6D_6): δ 6.7 (d, ^3J(PC) = 7.4 Hz, SiMe), 10.4 (d, ^3J(PC) = 4.0 Hz, SiMe), 17.9 (dt, ^1J(PC) = 20.2 Hz, ^3J(PC) = 2.1 Hz, PMe_3), 20.0 (ddd, ^1J(PC) = 28.7, ^3J(PC) = 1.3, 3.6 Hz, PMe_3), 20.7 (m, $SiCH_2$), 27.9 (m, PCH_2), 127.9 (d, J(PC) = 10.0 Hz), 128.4 (d, J(PC) = 7.7 Hz), 129.5 (d, J(PC) = 8.8 Hz), 129.8 (d, J(PC) = 6.6 Hz), 132.2 (d, ^2J(PC) = 8.9 Hz, *o*-Ph), 134.7 (d, ^2J(PC) = 11.1 Hz, *o*-Ph), 138.0 (dt, ^1J(PC) = 47.5 Hz, J(PC) = 7 Hz, *ipso*-Ph), 139.8 (dt, ^1J(PC) = 28.8 Hz, J(PC) = 4 Hz, *ipso*-Ph). $^{29}Si\{^1H\}$ NMR (59.6 MHz, C_6D_6): δ 40.4 (dddd, ^1J(RhSi) = 26.1 Hz, $^2J(P_{cis}Si)$ = 10.5, 8.2, 6.9 Hz). $^{31}P\{^1H\}$ NMR (121.5 MHz, C_6D_6): δ −25.1 (broad m, PMe_3 (*trans* to RhH)), −7.6 (ddd, $^2J(PP_{trans})$ = 364 Hz, ^1J(RhP) = 108 Hz, $^2J(PP_{cis})$ = 32 Hz, PMe_3 (*trans* to PPh_2)), 55.5 (ddd, $^2J(PP_{trans})$ = 364 Hz, ^1J(RhP) = 110 Hz, $^2J(PP_{cis})$ = 26 Hz, PPh_2). IR (KBr pellet, $\tilde{\nu}$/cm^{-1}): 2900 (s), 1953 (vs, ν(RhH)), 1432 (s). MS (70eV, DEI): *m*/*z* 562 (M^+, 19), 486 ($M^+ - PMe_3$, 100). Anal. Calc. for $C_{22}H_{39}ClP_3RhSi$: C, 46.94; H, 6.98. Found: C, 47.21; H, 6.99.

Reaction of RhH(Cl)[(κ^2*Si*,*P*)-$Me_2Si(CH_2)_2PPh_2$](PMe_3)$_2$ (1) with an excess amount of MeLi

A Pyrex NMR tube (5 mm o.d.) was charged with **1** (34 mg, 0.061 mmol), benzene-d_6 (0.7 mL) and MeLi (1.4 M ether solution, 0.1 mL, 0.14mmol). The NMR tube was connected to the vacuum line and was flame-sealed. The reaction was monitored by ^{1}H and ^{31}P NMR spectroscopy. The quick formation of a coordinatively unsaturated Rh[(κ^2*Si*,*P*)-$Me_2Si(CH_2)_2PPh_2$]-(PMe_3)$_2$ (**2**) was observed. However, **2** finally disappeared and the PMe_3 adduct of **2** Rh[(κ^2*Si*,*P*)-$Me_2Si(CH_2)_2PPh_2$](PMe_3)$_3$(**3**) was formed. The authentic syntheses and data of **2** and **3** are described below.

Reaction of RhH(Cl)[(κ^2*Si*,*P*)-$Me_2Si(CH_2)_2PPh_2$](PMe_3)$_2$ (1) with an excess amount of MeLi

Complex **1** (306.7 mg, 0.545 mmol) was placed in a Pyrex tube having a Teflon needle bulb at the top. The tube was attached to a vacuum line, and toluene (5 mL) was trap-to-trap-transferred into it. After the Teflon bulb was closed, the tube was detached from the vacuum line and attached to the Argon line. An ether solution of MeLi (1.14 M, 1.4 mL, 1.6 mmol) was added into the tube by syringe. The color of the solution immediately changed from light yellow to orange. After 10 min, the color of the solution became brown. The tube was attached to the vacuum line again, and the reaction mixture was concentrated to dryness and toluene (5 mL) was transferred into it. The tube was flame-sealed and unsealed in an N_2 glovebox. The reaction mixture was filtered through a Celite pad. The filtrate was concentrated and cooled to −75 °C to allow the growing of orange crystals which were collected by filtration to give Rh[(κ^2*Si*,*P*)-$Me_2Si(CH_2)_2PPh_2$](PMe_3)$_3$ (**3**) (98.4 mg, 0.163 mmol, 30%).

Rh[(κ^2*Si*,*P*)-$Me_2Si(CH_2)_2PPh_2$](PMe_3)$_2$ (2)

Complex **1** (237 mg, 0.420 mmol) was placed in a Pyrex tube (12 mm o.d.) having a Teflon needle valve at the top. The tube was attached to a vacuum line, and toluene (5 mL) was trap-to-trap-transferred into it. After the Teflon valve was closed, the tube was detached from the vacuum line and attached to an Argon line. An ether solution of MeLi (1.04 M, 0.45 mL, 0.47 mmol) was added into the tube by a syringe. The color of the solution immediately changed from light yellow to orange. The tube was attached to the vacuum line again and the reaction mixture was stirred under high vacuum for 5 min. Volatiles were removed and toluene (5 mL) was transferred into it. The tube was flame-sealed and unsealed in an N_2 glovebox. The reaction mixture was filtered through a Celite pad. The filtrate was concentrated to *ca.* 2 mL and cooled to −75 °C to allow the growing of orange crystals which were collected by filtration to give Rh[(κ^2*Si*,*P*)-$Me_2Si(CH_2)_2PPh_2$](PMe_3)$_2$ (**2**) (77 mg, 0.146 mmol, 35%). ^{1}H NMR (300 MHz, toluene-d_8, 20 °C): δ 0.58 (s, 6H, $SiMe_2$), 0.70 (m, 2H, $SiCH_2$), 1.08 (br., 18H, 2 × PMe_3), 2.32 (m, 2H, PCH_2), 7.02–7.09 (m, 6H, *m,p*-Ph), 7.86 (m, 4H, *o*-Ph). ^{1}H NMR (300 MHz, toluene-d_8, −40 °C): δ 0.80 (d, ^2J(PH) = 4.7 Hz, 9H, PMe_3), 0.86 (s, 6H, $SiMe_2$), 1.32 (d, ^2J(PH) = 5.7 Hz, 9H, PMe_3), 2.43 (m, 2H, PCH_2), 6.95–7.07, 8.00 (m, 10H, PPh_2). $^{13}C\{^1H\}$ NMR (75.5 MHz, C_6D_6, 20 °C): δ 7.9 (s, $SiMe_2$), 19.3 (m, $SiCH_2$), 21.4–21.7 (m, 2 × PMe_3), 35.2 (m, PCH_2), 129.0, 129.3 (s, *m,p*-Ph), 134.1 (d, ^2J(PC) = 13.0 Hz, *o*-Ph), 140.3 (d, ^1J(PC) = 24.6 Hz, *ipso*-Ph). $^{29}Si\{^1H\}$ NMR (59.6 MHz, toluene-d_8, 20 °C): δ 42.3 (m). $^{31}P\{^1H\}$ NMR (121.5 MHz, toluene-d_8, 20 °C): δ −14.8 (br. t, ^1J(RhP) = 130 Hz, 2 × PMe_3), 70.4 (dt, ^1J(RhP) = 160 Hz, ^2J(PP) = 131 Hz, PPh_2). $^{31}P\{^1H\}$ NMR (121.5 MHz, toluene-d_8, −40 °C): δ −21.1 (ddd, ^1J(RhP) = 113 Hz, ^2J(PP*cis*) = 35 Hz, PMe_3 (*trans* to $SiMe_2$, −9.0 (ddd, ^2J(PP*trans*) = 296 Hz, ^1J(RhP) = 148 Hz, $^2J(PP_{cis})$ = 36 Hz, PMe_3 (*trans* to PPh_2)), 70.5 (ddd, $^2J(PP_{trans})$ = 296 Hz, ^1J(RhP) = 157 Hz, ^2J(PP*cis*) = 36 Hz, PPh_2). Mass (70 eV, EI): *m*/*z* 526 (M^+, 43), 450 ($M^+ - PMe_3$, 100), 374 ($M^+ - 2PMe_3$, 20). IR (KBr pellet, $\tilde{\nu}$/cm^{-1}): 1419 (m), 1298 (w), 1144 (w), 949 (s), 696 (m). Anal. Calc. for $C_{22}H_{38}P_3RhSi$: C, 50.19; H, 7.28. Found: C, 49.77; H, 7.15.

Rh[(κ^2*Si*,*P*)-$Me_2Si(CH_2)_2PPh_2$](PMe_3)$_3$ (3)

Complex **1** (506 mg, 0.900 mmol) was placed in a round-bottomed flask (30 mL) having a Teflon needle valve at the top. The tube was attached to a vacuum line, and toluene (10 mL) was trap-to-trap-transferred into it. After the Teflon valve was closed, the tube was detached from the vacuum line and attached to an argon line. An ether solution of MeLi (1.04 M, 0.96 mL, 0.998 mmol) and PMe_3 (0.35 mL, 3.44 mmol) was added into the tube by a syringe under an argon atmosphere. The color of the solution immediately changed from light yellow to orange. The tube was attached to the vacuum line again, and the reaction mixture was stirred under high vacuum for 10 min. The resulting solution was concentrated to dryness. The tube was flame-sealed and unsealed in an N_2 glovebox. The residue was extracted with toluene (2 mL × 3) and the extract was filtered through a Celite pad. The filtrate was concentrated to *ca.* 2 mL and cooled to −75 °C to allow the growing of

Table 4 Crystallographic parameters of **1**, **2**, and **3**

	1	**2**	**3**
Formula	$C_{22}H_{39}SiP_3ClRh$	$C_{22}H_{38}SiP_3Rh$	$C_{25}H_{47}SiP_4Rh$
M	562.92	526.45	602.53
Crystal system	Orthorhombic	Triclinic	Orthorhombic
a/Å	15.1621(8)	11.4349(6)	11.8518(3)
b/Å	25.695(1)	12.9113(9)	35.8507(8)
c/Å	13.5872(6)	9.5714(4)	14.0432(2)
α/°	90	100.379(5)	90
β/°	90	104.093(2)	90
γ/°	90	106.562(3)	90
V/Å^3	5293.5(4)	1265.5(1)	5966.9(4)
Space group	*Pbca*	$P\bar{1}$	*Pccn*
Z	8	2	8
d_{calc}/g cm^{-3}	1.413	1.381	1.341
Crystal size/mm	0.20 × 0.20 × 0.05	0.20 × 0.20 × 0.10	0.10 × 0.10 × 0.10
μ(Mo Kα)/cm^{-1}	9.78	9.16	8.38
2θ max/°	55	55	55
T/K	150	150	150
No. of reflections measured	22911	11725	23536
No. of unique data (R_{int})	6018 (0.056)	5596 (0.047)	6620 (0.026)
No. of params	257	244	280
Residuals: *R*; *Rw* (all data)	0.077; 0.215	0.068; 0.189	0.061; 0.119
Residuals; *R*1 ($I > 2\sigma(I)$)	0.048	0.037	0.035
No. of reflections to calc. *R*1	5110	5481	4709

$R = \Sigma(F_o^2 - F_c^2)/\Sigma F_o^2$, $Rw = [\Sigma w(F_o^2 - F_c^2)^2/\Sigma w(F_o^2)^2]^{1/2}$ $R1 = \Sigma\left||F_o| - |F_c|\right|/\Sigma|F_o|$ for $I > 2.0\sigma(I)$.

orange crystals which were collected by filtration to give Rh[(κ^2*Si*,*P*)-$Me_2Si(CH_2)_2PPh_2$]$(PMe_3)_3$ (**3**) (402 mg, 0.667 mmol, 74%). ^{1}H NMR (300 MHz, toluene-d_8, 20 °C): δ 0.53 (s, 6H, $SiMe_2$), 0.67–1.07 (br., 29 H, $SiCH_2$ and 3 × PMe_3), 2.42 (m, 2H, PCH_2), 7.05–7.13 (m, 6H, *m*,*p*-Ph), 7.66 (m, 4H, *o*-Ph). ^{1}H NMR (300 MHz, toluene-d_8, −30 °C): δ 0.65 (d, ^2J(PH) = 5.3 Hz, 9H, PMe_3 (axial)), 0.81 (s, 6H, $SiMe_2$), 1.32 (s, 18H, 2 × PMe_3 (equatorial)), 2.57 (m, 2H, PCH_2), 6.99–7.16 (m, 6H, *m*,*p*-Ph), 7.74 (m, 4H, *o*-Ph). ^{13}C{^{1}H} NMR (75.5 MHz, toluene-d_8, 20 °C): δ 10.2 (s, $SiMe_2$), 23.0 (d, ^2J(PC) = 42.9 Hz, $SiCH_2$), 23.7–27.8 (br, 3 × PMe_3), 35.9 (d, ^1J(PC) = 27.6 Hz, PCH_2), 134.0 (d, ^2J(PC) = 13.8 Hz, *o*-Ph), 144.9 (m, *ipso*-Ph). ^{31}P{^{1}H} NMR (121.5 MHz, toluene-d_8, 20 °C): δ −24.0 (br., 2 × PMe_3), −13.9 (br., PMe_3), 65.8 (br., PPh_2). ^{31}P{^{1}H} NMR (121.5 MHz, toluene-d_8, −30 °C): δ −22.8 (ddd, ^1J(RhP) = 154 Hz, ^2J(PP) = 48, 116 Hz, 2 × PMe_3 (equatorial)), −13.1 (dq, ^1J(RhP) = 95 Hz, ^2J(PP) = 48 Hz, PMe_3 (axial)), 65.7 (dtd, ^1J(RhP) = 159 Hz, ^2J(PP) = 116 Hz, ^2J(PP) = 48 Hz, PPh_2). Mass (70 eV, DEI): *m*/*z* 526 ($M^+ - PMe_3$, 37), 450 ($M^+ - 2PMe_3$, 100), 374 ($M^+ - 3PMe_3$, 22). IR (KBr pellet, $\tilde{\nu}$/cm^{-1}): 1432 (m), 1294 (w), 1151 (vw), 948 (s), 809 (m), 736 (m), 698 (m), 516 (m). Anal. Calc for $C_{25}H_{47}P_4RhSi$: C, 49.84; H, 7.86. Found: C, 49.73; H, 7.62.

Variable temperature NMR of Rh[(κ^2*Si*,*P*)-$Me_2Si(CH_2)_2PPh_2$]$(PMe_3)_3$ (3) and PMe_3

A Pyrex NMR tube (5 mm o.d.) was charged with **3** (14 mg, 0.0232 mmol) and PMe_3 (5 μL, 0.0492 mmol), and toluene-d_8 (0.6 mL) was introduced into this tube under high vacuum by the trap-to-trap-transfer technique. The NMR tube was flame-sealed. The dynamic behavior of PMe_3 ligands was monitored by ^{31}P NMR spectroscopy.

X-Ray crystal structure determination of 1, 2, and 3

Intensity data for X-ray crystal structure analysis were collected at 150 K on a Rigaku RAXIS-RAPID Imaging Plate diffractometer with graphite-monochromated Mo Kα radiation. A total of 44 images, corresponding to 220.0° oscillation angles, were collected with 2 different goniometer settings. Exposure time was 0.50 minutes per degree. Readout was performed in the 0.100 mm pixel mode. For **1** and **2**, numerical absorption corrections were applied on each crystal shape. The structures were solved by Patterson methods (PATTY) and refined by the least-squares technique. All non-hydrogen atoms were located and refined anisotropically. The coordinates of a hydrogen atoms connected to Rh in 1 were determined by the difference Fourier synthesis and refined isotropically. Other hydrogen atoms were placed at their geometrically calculated positions. Data reduction and refinement were performed using teXsan software packages. Crystallographic data of **1**, **2**, and **3** are listed in Table 4.

CCDC reference numbers 173810–173812.

See http://www.rsc.org/suppdata/dt/b2/b201208c/ for crystallographic data in CIF or other electronic format.

Reaction of Rh[(κ^2*Si*,*P*)-$Me_2Si(CH_2)_2PPh_2$]$(PMe_3)_2$ (2) with $HSiMe_2Ph$

A Pyrex NMR tube was charged with **2** (9 mg, 0.017 mmol), $HSiMe_2Ph$ (15 μL, 0.098 mmol) and C_6Me_6 (1 mg, internal standard), and benzene-d_6 (0.7 mL) was introduced to this tube under high vacuum by the trap-to-trap-transfer technique. This tube was flame-sealed. The reaction was monitored by NMR spectroscopy and proceeded spontaneously at room temperature to give $RhH(SiMe_2Ph)$[(κ^2*Si*,*P*)-$Me_2Si(CH_2)_2PPh_2$]$(PMe_3)_2$ (**4**) quantitatively. When the reaction was continued at room temperature for 20 h, the mixture of **4** and $HSiMe_2Ph$ were converted to RhH_2[(κ^2*Si*,*P*)-$Me_2Si(CH_2)_2PPh_2$]$(PMe_3)_2$ (**5**) and $(SiMe_2Ph)_2$ in 91% yield each. Data of $RhH(SiMe_2Ph)$-[(κ^2*Si*,*P*)-$Me_2Si(CH_2)_2PPh_2$]$(PMe_3)_2$ (**4**): ^{1}H NMR (300 MHz, toluene-d_8, −20 °C): δ −10.30 (dq, $^2J(P_{trans}H)$ = 123 Hz, $^2J(P_{cis}H) = {}^1J$(RhH) = 16 Hz, 1H, RhH), 0.45 (s, 6H, $SiMe_2Ph$), 0.55 (m, 2H, $SiCH_2$), 0.64, 0.68 (s, 3H × 2, CH_2SiMe_2), 0.76 (d, ^2J(PH) = 5.9 Hz, 9H, PMe_3), 0.90 (d, ^2J(PH) = 6.5 Hz, 9H, PMe_3), 2.00 (m, 2H, PCH_2), 6.91, 7.55, 7.66 (m, Ph). ^{31}P{^{1}H} NMR (121.5 MHz, toluene-d_8, 20 °C): δ −28.3 (ddd, ^1J(RhP) = 80 Hz, $^2J(PP_{cis})$ = 29, 32 Hz, PMe_3), −18.2 (ddd, ^1J(RhP) = 103 Hz, $^2J(PP_{cis})$ = 25, 29 Hz, PMe_3), 60.1 (ddd, ^1J(RhP) = 82 Hz, $^2J(PP_{cis})$ = 25, 32 Hz, PPh_2).

Rh[(κ^2*Si*,*P*)-$Me_2Si(CH_2)_2PPh_2$]$(PMe_3)_2$ (3) with $HSiMe_2Ph$

A Pyrex NMR tube was charged with **3** (11 mg, 0.018 mmol), $HSiMe_2Ph$ (15 μL, 0.098 mmol) and C_6Me_6 (1 mg, internal standard), and benzene-d_6 (0.7 mL) was introduced to this tube under high vacuum by the trap-to-trap-transfer technique. This

tube was flame-sealed. The reaction was monitored by NMR spectroscopy which confirmed the quick formation of the mixture of **3**, **4**, and free PMe_3. The prolonged reaction at room temperature did not cause any change in the ratio of products. In the course of the reaction, a trace amount of $(SiMe_2Ph)_2$ was confirmed. Heating the resulting mixture at 80 °C gave rise to decomposition of complexes **3** and **4**.

Synthesis of $RhH_2[(\kappa^2Si,P)\text{-}Me_2Si(CH_2)_2PPh_2](PMe_3)_2$ (5)

H_2 gas was bubbled through a toluene solution (3 mL) of **3** (60 mg, 0.010 mmol) at room temperature for 20 min. The color gradually changed from orange to light yellow. Evaporation of the resulting solution, followed by the addition of pentane (0.5 mL) precipitated a light yellow solid. The solid was washed by pentane (0.5 mL × 3) to give **5** (33 mg, 0.062 mmol, 63%) as a light yellow powder. ^{1}H NMR (300 MHz, toluene-d_8) δ −10.57 (dq, $^2J(P_{trans}H)$ = 135 Hz, $^2J(P_{cis}H)$ = ^1J(RhH) = 18 Hz, 1H, RhH), −9.27 (dq, $^2J(P_{trans}H)$ = 135 Hz, $^2J(P_{cis}H)$ = ^1J(RhH) = 21 Hz, 1H, RhH), 0.61, 0.83 (s, 3H, SiMe), 0.76–1.20 (m, 1H × 2, $SiCH_2$), 0.84 (d, ^2J(PH) = 6.3 Hz, 9H, PMe_3), 1.15 (d, ^2J(PH) = 6.0 Hz, 9H, PMe_3), 1.82, 2.36 (m, 2H, PCH_2), 6.95–7.14 (m, 6H, *m,p*-Ph), 7.48, 7.67 (m, 4H, *o*-Ph). $^{31}P\{^1H\}$ NMR (121.5 MHz, toluene-d_8) δ −20.0 (ddd, ^1J(PRh) = 88 Hz, ^2J(PP) = 29 Hz, ^2J(PP) = 19 Hz, PMe_3), −11.3 (dt, ^1J(PRh) = 101 Hz, ^2J(PP) = 27 Hz, PMe_3), 68.2 (dt, ^1J(PRh) = 101.1 Hz, ^2J(PP) = 22 Hz, PPh_2). Mass (70 eV, DEI): *m*/*z* 526 (M^+-2H, 100), 450 (M^+-2H–PMe_3, 44). IR (KBr pellet, $\tilde{\nu}$/cm^{-1}): 2362 (s), 2337 (s), 1926, 1884 (s, ν(RhH)), 939 (s). Anal. Calc. for $C_{22}H_{40}SiP_3Rh$: C, 50.00; H, 7.63%. Found: C, 49.29; H, 7.44%.

Acknowledgements

This work was supported by Grants-in-Aid for Scientific Research (Nos. 11740367, 12640533, and 13029012) from the Ministry of Education, Culture, Sports, Science and Technology, Japan and financial support from the Nissan Science Foundation, Inoue Foundation for Science, and Tokuyama Science Foundation. We thank Shin-Etsu Chemical Co., Ltd., and Toray Dow Corning Silicone Co., Ltd., for their gifts of silicon compounds.

References

1 J. A. Osborn, F. H. Jardine, J. F. Young and G. Wilkinson, *J. Chem. Soc, A*, 1966, 1711.
2 (*a*) J. Chatt, C. Eaborn and S. Ibekwe, *Chem. Commun.*, 1966, 700; (*b*) R. McWeeny, R. Mason and A. D. C. Towl, *Discuss. Faraday Soc.*, 1969, **47**, 20; (*c*) R. N. Haszeldine, R. V. Parish and J. H. Setchfield, *J. Organomet. Chem.*, 1973, **57**, 279; (*d*) L. A. Latif, C. Eaborn and A. P. Pidcock, *J. Organomet. Chem.*, 1994, **474**, 217; (*e*) P. Kapoor, K. Lovqvist and A. Oskarsson, *Acta Crystallogr., Sect. C*, 1995, **51**, 611.
3 F. L. Joslin and S. R. Stobart, *J. Chem. Soc., Chem. Commun.*, 1989, 504.
4 M. Aizenberg and D. Milstein, *Science*, 1994, **265**, 359.
5 D. L. Thorn and R. L. Harlow, *Inorg. Chem.*, 1990, **29**, 2017.
6 M. Okazaki, S. Ohshitanai, M. Iwata, H. Tobita and H. Ogino, *Coord. Chem. Rev.*, 2002, **226**, 167.
7 M. Okazaki, S. Ohshitanai, H. Tobita and H. Ogino, *Chem. Lett.*, 2001, 952.
8 (*a*) K. Osakada, T. Koizumi, S. Sarai and T. Yamamoto, *Organometallics*, 1998, **17**, 1868; (*b*) K. Osakada, S. Sarai, T. Koizumi and T. Yamamoto, *Organometallics*, 1997, **16**, 3973.
9 S. L. Grundy, R. D. Holmes-Smith, S. R. Stobart and M. A. Williams, *Inorg. Chem.*, 1991, **30**, 3333.
10 R. T. Price, R. A. Andersen and E. L. Muetterties, *J. Organomet. Chem.*, 1989, **376**, 407.
11 (*a*) M. Aizenberg, J. Ott, C. L. Eisevier and D. Milstein, *J. Organomet. Chem.*, 1998, **551**, 81; (*b*) P. Hofmann, C. Meier, W. Hiller, M. Heckel, J. Riede and M. U. Schmidt, *J. Organomet. Chem.*, 1995, **490**, 51.
12 D. L. Lichtenberger and A. Rai-Chaudhuri, *J. Am. Chem. Soc.*, 1991, **113**, 2923.
13 (*a*) S. Sun and D. A. Sweigart, *Adv. Organomet. Chem.*, 1996, **40**, 171; (*b*) M. Yuki, T. Mitsui, S. Inomata, M. Okazaki and H. Ogino, *Chem. Lett.*, 1998, 561.
14 G. P. Mitchell and T. D. Tilley, *Organometallics*, 1998, **17**, 2912.
15 D. L. Thorn, *Organometallics*, 1982, **1**, 197.
16 M. Okazaki, H. Tobita and H. Ogino, *Organometallics*, 1996, **15**, 2790.
17 T. Ziegler, V. Tschinke and C. Ursenbach, *J. Am. Chem. Soc.*, 1987, **109**, 4825.
18 F. A. Cotton and G. Wilkinson, *Advanced Inorganic Chemistry*, John Wiley and Sons, New York, 1988, p. 777.
19 H. Nagashima, K. Tatebe, T. Ishibashi, J. Sakakibara and K. Itoh, *Organometallics*, 1995, **14**, 2868.
20 (*a*) H. Tobita, K. Hasegawa, J. J. G. Minglana, L.-S. Luh, M. Okazaki and H. Ogino, *Organometallics*, 1999, **18**, 2058; (*b*) J. J. G. Minglana, M. Okazaki, H. Tobita and H. Ogino, *Chem. Lett.*., 2002, 406.
21 (*a*) J. Y. Corey, *Advances in Silicon Chemistry*, ed. G. Larson, JAI Press Inc., Greenwich, 1991, vol. 1, p. 327; (*b*) M. D. Curtis and P. S. Epstein, *Adv. Organomet. Chem.*, 1981, **19**, 213.
22 H. Gilman and G. D. Lichtenwalter, *J. Am. Chem. Soc.*, 1958, **80**, 608.
23 R. D. Holmes-Smith, R. D. Osei and S. R. Stobart, *J. Chem. Soc., Perkin Trans.*, 1983, 861.
24 J. A. Osborn and G. Wilkinson, *J. Chem. Soc. A*, 1968, 1054.